


Observation of the $^1S_0 \rightarrow ^3P_0$ Clock Transition in $^{27}\text{Al}^+$

T. Rosenband,^{1,*} P. O. Schmidt,^{1,†} D. B. Hume,¹ W. M. Itano,¹ T. M. Fortier,² J. E. Stalnaker,¹ K. Kim,^{1,‡} S. A. Diddams,¹
J. C. J. Koelemeij,^{1,§} J. C. Bergquist,¹ and D. J. Wineland¹

¹National Institute of Standards and Technology, 325 Broadway, Boulder, Colorado 80305, USA

²P-23 Physics Division, Los Alamos National Laboratory, Los Alamos, New Mexico 87545, USA

(Received 6 March 2007; published 31 May 2007)

We report, for the first time, laser spectroscopy of the $^1S_0 \rightarrow ^3P_0$ clock transition in $^{27}\text{Al}^+$. A single aluminum ion and a single beryllium ion are simultaneously confined in a linear Paul trap, coupled by their mutual Coulomb repulsion. This coupling allows the beryllium ion to sympathetically cool the aluminum ion and also enables transfer of the aluminum's electronic state to the beryllium's hyperfine state, which can be measured with high fidelity. These techniques are applied to measure the clock transition frequency $\nu = 1\,121\,015\,393\,207\,851(6)$ Hz. They are also used to measure the lifetime of the metastable clock state $\tau = 20.6 \pm 1.4$ s, the ground state 1S_0 g factor $g_S = -0.000\,792\,48(14)$, and the excited state 3P_0 g factor $g_P = -0.001\,976\,86(21)$, in units of the Bohr magneton.

DOI: [10.1103/PhysRevLett.98.220801](https://doi.org/10.1103/PhysRevLett.98.220801)

PACS numbers: 06.30.Ft, 32.10.Dk, 32.70.Cs, 39.30.+w

The $^1S_0 \rightarrow ^3P_0$ transition in Al^+ has long been recognized as a good clock transition [1,2], due to its narrow natural linewidth (8 mHz) and its insensitivity to magnetic fields and electric field gradients, which are common in ion traps. More recently, this transition was also found to have a small room-temperature blackbody radiation shift [3]. However, difficulties with direct laser cooling and state detection have so far prevented its use.

Some of the basic ingredients for ion-trap-based quantum computing [4] can be used to overcome these difficulties with the method of quantum logic spectroscopy (QLS) [5], where an auxiliary ion takes over the requirements of laser cooling and state detection. QLS was first demonstrated experimentally on the $^1S_0 \rightarrow ^3P_1$ transition in $^{27}\text{Al}^+$ [6]. Here we use this technique for spectroscopy of the narrow $^1S_0 \rightarrow ^3P_0$ clock transition, allowing, for the first time, high precision optical spectroscopy of an atomic species that cannot be directly laser cooled.

With the advent of octave-spanning Ti:sapphire femtosecond laser frequency combs (FLFCs) [7,8], optical atomic frequency standards can be compared with an uncertainty limited only by quantum projection noise [9] and the systematic errors of the atomic standards. This stability and accuracy can be transferred to any part of the optical spectrum, as well as the rf domain. The $^1S_0 \rightarrow ^3P_0$ clock transition in $^{27}\text{Al}^+$, due to its insensitivity to external fields, is a viable candidate to reach 10^{-18} inaccuracy. Here we demonstrate high precision spectroscopy of the clock transition in a single $^{27}\text{Al}^+$ ion, which is the fundamental step necessary to realize such a frequency standard.

With nuclear spin $I = \frac{5}{2}$, $^{27}\text{Al}^+$ has no first-order magnetic-field-independent transition, but this is not a significant drawback. Instead, we create a “virtual” ($^1S_0, m_F = 0$) \rightarrow ($^3P_0, m_{F'} = 0$) field-independent transition, by regularly alternating between ($m_F = -\frac{5}{2}$) \rightarrow

($m_{F'} = -\frac{5}{2}$) and ($m_F = \frac{5}{2}$) \rightarrow ($m_{F'} = \frac{5}{2}$) transitions [10]. This way, the average Zeeman state of both the ground and the excited clock states is strictly zero. A benefit of this approach is that the outer $m_F = \pm\frac{5}{2}$ states can be prepared more easily than the inner m_F states, by optical pumping through the ($^3P_1, F = \frac{7}{2}$) state (300 μs lifetime). In addition, the ion's Zeeman splitting serves as a real-time magnetometer to determine the quadratic Zeeman shift of the clock transition.

A single $^9\text{Be}^+$ and a $^{27}\text{Al}^+$ ion are loaded into a linear Paul trap [11], by electron impact ionization. Under ultrahigh vacuum conditions, one ion pair usually lasts for several hours, before an adverse chemical reaction with background gas removes one of the ions from the trap. The pair forms a two-ion “crystal” along the trap axis, whose in-phase-motion axial normal mode frequency is 2.62 MHz. The radial modes (perpendicular to the trap axis), where the $^{27}\text{Al}^+$ ion's amplitude is largest, have frequencies of 3.8 and 4.9 MHz. Laser beams of 313 nm wavelength drive Doppler-cooling, stimulated Raman, and repumping transitions on $^9\text{Be}^+$ [12]. Another laser produces 267.0 nm radiation to drive the ($^1S_0, F = \frac{5}{2}$) \rightarrow ($^3P_1, F = \frac{7}{2}$) transition in $^{27}\text{Al}^+$, and a frequency-quadrupled fiber laser at 267.4 nm, with approximately 3 Hz linewidth, excites the clock transition.

The $^1S_0 \rightarrow ^3P_0$ transition is probed with single interrogation pulses from the clock laser. Since the upper state is metastable, the method of electron-shelving detection [1] is applied. This way the $^1S_0 \rightarrow ^3P_1$ transition is modulated by the clock states, and the modulation condition (allowed or forbidden) is detected with quantum logic.

QLS of the $^1S_0 \rightarrow ^3P_1$ transition has been described previously [6] and is used similarly here. A pulse sequence (described below and shown in Fig. 1) maps the $^{27}\text{Al}^+$ 1S_0 state to the dark $^9\text{Be}^+$ $F = 1$ hyperfine ground state via a $^1S_0 \rightarrow ^3P_1$ motional-sideband excitation. This sequence is

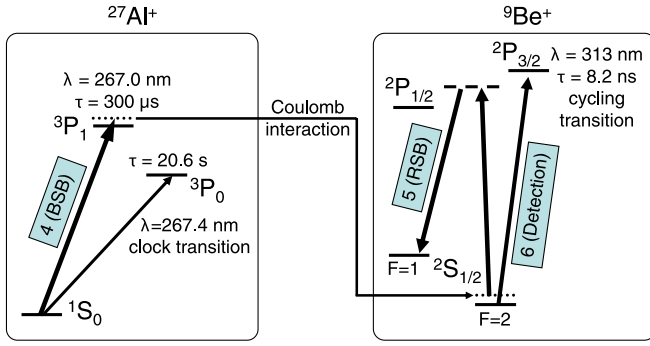


FIG. 1 (color online). Transfer of the $^{27}\text{Al}^+$ clock state to $^9\text{Be}^+$ for detection. Quantum state transfer proceeds according to numbers 4, 5, and 6 in shaded boxes, which denote corresponding steps in the text. Dotted lines denote the first vibrational excitation of the in-phase axial mode. The dashed line represents the virtual level of the $^9\text{Be}^+$ stimulated Raman transition.

blocked when the $^{27}\text{Al}^+$ ion is in the 3P_0 state, leaving $^9\text{Be}^+$ in the bright $F = 2$ hyperfine ground state, into which it had previously been optically pumped. An average of seven $^9\text{Be}^+$ 313 nm fluorescence photons are counted if the $^{27}\text{Al}^+$ ion is in the 3P_0 state [Fig. 2(b)], and only one photon is counted if the $^{27}\text{Al}^+$ ion is in the 1S_0 state [Fig. 2(a)]. This provides for clock-state discrimination with 80% fidelity in a single detection experiment, limited by inaccuracies in the various π pulses, and imperfect ground-state cooling. However, the single-experiment detection fidelity does not significantly affect the final detection fidelity for the clock state. We simply repeat the readout sequence several times, and the combined information allows nearly unit detection fidelity [13].

A typical ($^1S_0, m_F = \frac{5}{2}$) \rightarrow ($^3P_0, m_{F'} = \frac{5}{2}$) interrogation consists of the following steps, with specified durations. For $m_F = m_{F'} = -\frac{5}{2}$, the polarizations and angular momentum states of $^{27}\text{Al}^+$ are reversed. (i) Sympathetic Doppler cooling via $^9\text{Be}^+$ (600 μs) cools all six normal modes of the two-ion crystal to the Doppler limit (mean motional quantum number $\bar{n} \approx 3$). (ii) Clock interrogation (1–100 ms pulse duration, adjusted for desired resolution) drives the $^1S_0 \rightarrow ^3P_0$ transition. Beryllium Doppler-cooling light is applied simultaneously to counteract anomalous heating of the ions [14,15].

Subsequently, state detection (1S_0 or 3P_0) is performed by repeating the following sequence about 10 times. (1) Optical pumping π -pulse $^{27}\text{Al}^+$ ($^1S_0, F = \frac{5}{2}, m_F = \frac{3}{2}$) \rightarrow ($^3P_1, F = \frac{7}{2}, m_{F'} = \frac{5}{2}$) (4 μs) transfers the residual inner Zeeman state population to the outer $m_F = \frac{5}{2}$ state. The inner states may be populated due to spontaneous decay from the 3P_0 state or due to imperfect polarization and off-resonant transitions during other $^1S_0 \rightarrow ^3P_1$ pulses. Most of the time this pulse has no effect, because $^{27}\text{Al}^+$ is already in the ($^1S_0, m_F = \frac{5}{2}$) state. (2) Sympathetic Doppler cooling (600 μs). (3) Ground-state cooling of

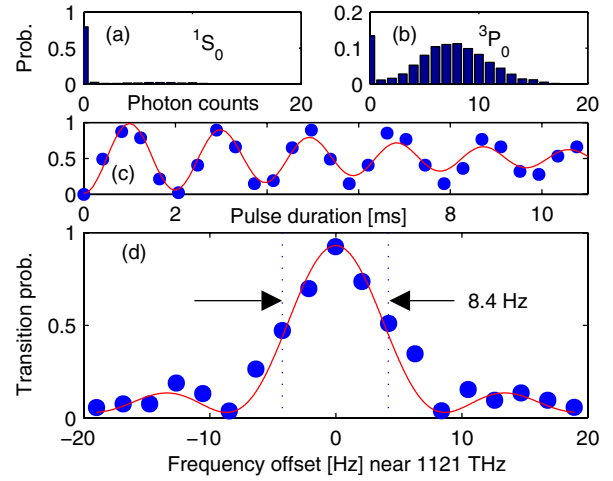


FIG. 2 (color online). Histograms of photon counts used for discrimination of (a) 1S_0 and (b) 3P_0 states in $^{27}\text{Al}^+$ via $^9\text{Be}^+$ fluorescence (see text). (c) Rabi flopping averaged over 40 scans of the $^1S_0 \rightarrow ^3P_0$ probe time (0–11 ms). The smooth line represents predicted Rabi flopping with damping due to fluctuating Debye-Waller factors [28]. (d) Average transition probability of 50 frequency scans across the ($^1S_0, m_F = \frac{5}{2}$) \rightarrow ($^3P_0, m_{F'} = \frac{5}{2}$) resonance in $^{27}\text{Al}^+$. Each measurement consists of one 3P_0 interrogation (100 ms probe time), followed by 5–10 state-detection repetitions (10–20 ms total). The fitted curve is a Fourier-limited Rabi line shape, scaled to the observed 90% contrast.

the axial modes of the two-ion crystal (1 ms), $\bar{n} < 0.05$ [16]. (4) Blue sideband (BSB) π -pulse $^{27}\text{Al}^+$ ($^1S_0, F = \frac{5}{2}, m_F = \frac{5}{2}$) \rightarrow ($^3P_1, F = \frac{7}{2}, m_{F'} = \frac{7}{2}$) (30 μs). (5) Red sideband (RSB) π -pulse $^9\text{Be}^+$ ($^2S_{1/2}, F = 2, m_F = -2$) \rightarrow ($^2S_{1/2}, F = 1, m_F = -1$) (7 μs). (6) Detection via the $^9\text{Be}^+$ cycling transition (200 μs) ($^2S_{1/2}, F = 2, m_F = -2$) \rightarrow ($^2P_{3/2}, F = 3, m_F = -3$). In the $F = 2$ state, $^9\text{Be}^+$ fluoresces strongly, and it is dark in the $F = 1$ state [Figs. 2(a) and 2(b)].

Because the duration of each state-detection repetition is about 2 ms, excitations into the 3P_1 state (300 μs lifetime) usually decay back to the 1S_0 state, allowing reexcitation, while 3P_0 excitations (20.6 s lifetime) are unlikely to change during the detection sequence.

For every clock interrogation pulse, the sequence of photon counts in step 6 is recorded by a computer, which performs a maximum-likelihood analysis to determine whether the $^{27}\text{Al}^+$ ion was in the 1S_0 or the 3P_0 state [13]. Transitions between the two states are detected, and multiple repetitions of the same experiment yield the transition probability. It should be noted that the ion may be in the 1S_0 or the 3P_0 state at the beginning of each experiment, depending on the outcome of the previous experiment [17]. The final signal is the computer's determination of whether or not the ion has made a transition. Figures 2(c) and 2(d) show Rabi flopping and a scan of the clock laser

frequency across the $^1S_0 \rightarrow ^3P_0$ resonance with this method.

When performing an absolute frequency measurement of the $^1S_0 \rightarrow ^3P_0$ transition, the linear Zeeman splitting of several 10^4 Hz/mT (see below) in both the ground and the excited clock states must be accounted for. To achieve first-order field insensitivity, we create a virtual $m_F = 0$ transition by alternating between states of opposite angular momentum and tracking separately the mean and difference frequencies of the two transitions [10]. The mean frequency has no linear dependence on the magnetic field, although a quadratic Zeeman shift of -70 Hz/mT² remains [18]. The difference frequency is directly proportional to the magnetic field, providing a real-time field measurement. In this way, the linear Zeeman effect does not shift the clock's center frequency, while the quadratic Zeeman shift can be determined from the linear splitting and accounted for with submillihertz inaccuracy.

To lock the laser frequency to the atomic reference, the laser's frequency offset from the atomic resonance is regularly measured and corrected. Frequency corrections are obtained by alternating between the left and right "half-power" points of the ion's resonance and applying frequency feedback to keep the transition probabilities equal. In order to switch between angular momentum states, a computer-controlled wave plate selects a purely σ_+ - or σ_- -polarized $^1S_0 \rightarrow ^3P_1$ light that optically pumps $^{27}\text{Al}^+$ to the $m_F = \pm \frac{5}{2}$ ground states. At the operating field of approximately 0.1 mT, and typical Fourier-limited linewidths of 20 Hz or less, the linear Zeeman structure of both clock states is well resolved. A synthesizer-driven acousto-optic frequency shifter changes the probe frequency by $\Delta f \approx -4$ kHz to drive the $(^1S_0, m_F = \frac{5}{2}) \rightarrow (^3P_0, m_{F'} = \frac{5}{2})$ transition and by $-\Delta f$ to drive the opposite Zeeman states. When locking the clock laser to the atomic transition, the clock ground state is switched between the $m_F = \pm \frac{5}{2}$ states every three seconds. This way, magnetic field fluctuations (typically below 100 nT in several minutes) contribute only short-term instability in the clock frequency rather than long-term inaccuracy.

We have locked the clock laser to the virtual $m_F = 0$ clock transition as described above and used the fourth subharmonic at 1070 nm to reference one tooth of an octave-spanning Ti:sapphire FLFC [19]. The offset frequency of the FLFC is locked by use of an f-2f interferometer, and the repetition rate is measured by a hydrogen maser, which is periodically (typically every 4 months) calibrated by the NIST-F1 primary cesium standard [20]. A 2600 s long measurement of the $^{27}\text{Al}^+$ clock transition frequency yields $\nu = 1\,121\,015\,393\,207\,851(6)$ Hz, where the uncertainty is dominated by short-term frequency fluctuations in the hydrogen maser [21]. Systematic uncertainties in $^{27}\text{Al}^+$ are not expected to be significant at this level, where the largest terms are second-order Doppler shifts of approximately 0.03 Hz.

We have also measured the Landé g factors of the 1S_0 and 3P_0 states. Interrogation pulses (π -polarized) yield the g -factor difference $g_P - g_S$ [22], where g_P and g_S are the g factors of the 3P_0 and 1S_0 states, respectively. In addition, we use σ_{\pm} -polarized interrogation pulses to measure another, linearly independent combination of g_P and g_S , providing an accurate measurement of both g factors, which is unaffected by the chemical shifts that currently limit the accuracy of nuclear magnetic resonance (NMR)-based measurements of g_S [23]. An external magnetic field B splits the $m_F = \pm \frac{5}{2}$, $\Delta m_F = 0$ transition frequencies by $\Delta\nu = 5B(g_P - g_S)\mu_B$, where μ_B is the Bohr magneton. The frequency splitting $\Delta\nu$ is tracked and recorded automatically in the clock laser lock described above. In order to measure the magnetic field, we use the simultaneously trapped $^9\text{Be}^+$ ion. $^9\text{Be}^+$ has well-known ground-state Zeeman splitting [24], allowing for accurate calibration of the external magnetic field. In between aluminum clock interrogations, a 1.25 GHz magnetic field is applied to the beryllium ion with a loop antenna. Computer control software adjusts the radiation frequency to drive and track the magnetic-field-sensitive $(^2S_{1/2}, F = 2, m_F = -2) \rightarrow (^2S_{1/2}, F = 1, m_F = -1)$ transition, establishing a record of the magnetic field. We find the Zeeman splitting of $^{27}\text{Al}^+$ to be $\Delta\nu/B = -82\,884(5)$ Hz/mT, or $g_P - g_S = -0.001\,184\,37(8)$ [Fig. 3(a)]. A recent multiconfiguration Dirac-Hartree-Fock calculation [18] yields a similar theoretical value of $g_P - g_S = -0.001\,18(6)$.

In order to determine separate values g_P and g_S , we repeated the above experiment with σ_{\pm} -polarized clock radiation. This way, the $(^1S_0, m_F = -\frac{5}{2}) \rightarrow (^3P_0, m_{F'} = -\frac{3}{2})$ and $(^1S_0, m_F = \frac{5}{2}) \rightarrow (^3P_0, m_{F'} = \frac{3}{2})$ transitions are probed, and their magnetic-field-induced splitting $\Delta\nu'$ is measured. From $\Delta\nu'/B = (3g_P - 5g_S)\mu_B = -27\,547(5)$ Hz/mT, we find $g_P = -0.001\,976\,86(21)$ and $g_S = -0.000\,792\,48(14)$. The uncertainties of these values are dominated by inaccuracies in the $^9\text{Be}^+$ -based magnetic field calibration. This was caused by a perturbation of the current supply for the dc magnetic field from the 1.25 GHz rf pulse itself. We estimate that this perturbation

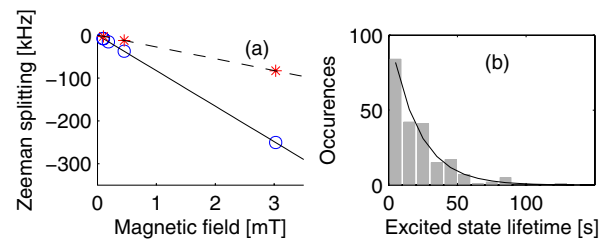


FIG. 3 (color online). (a) Linear Zeeman splitting of the $(m_F = \pm \frac{5}{2}) \rightarrow (m'_{F'} = \pm \frac{5}{2})$ transition pair (O) and the $(m_F = \pm \frac{5}{2}) \rightarrow (m'_{F'} = \pm \frac{3}{2})$ transition pair (*). Straight lines correspond to the reported g -factor differences. (b) Histogram of lifetimes of 215 decays from the 3P_0 state. The curve shows the expected number of decays for a lifetime $\tau = 20.6$ s.

is 21 ± 200 nT in both the π and the σ_{\pm} measurements and derive the stated uncertainties from the measurements at 3 mT, where the magnetic field uncertainty has the smallest effect on our results.

Since g_S depends solely on the ion's shielded nuclear magnetic moment, this measurement may be compared with the value recorded in nuclear data tables, which is derived from NMR experiments. An estimated shielding factor of $\sigma = 7.87(39) \times 10^{-4}$ [18] for $^{27}\text{Al}^+$ leads to a bare moment of $\mu_N = 3.64067(28)$ nuclear magnetons. This differs from the published value of $\mu_N = 3.64150687(65)$ [25] by $0.00084(28)$. However, the liquid-state NMR result does not account for the chemical shift of the nuclear magnetic moment due to the aqueous solution, which generally has a magnitude of 10^{-4} – 10^{-3} nuclear magnetons [23].

Hyperfine-induced spontaneous decay rates of 3P_0 states for the Mg-isoelectronic sequence have been calculated [26]. More recently, the $^{27}\text{Al}^+ ^3P_0$ lifetime was calculated [18] as 22.7 ± 4 s. Here we measured the lifetime by repeatedly exciting the 3P_0 state and waiting for spontaneous decay into the ground state [27]. The aluminum internal state was monitored by continuously applying the previously described clock-state readout sequence. Once decay has been detected, the ion is reexcited. A total of 215 spontaneous emission events were observed this way, with a mean lifetime $\tau = 20.6 \pm 1.4$ s. The reported uncertainty is statistical, and systematic biases are estimated to be less than 0.25 s. Figure 3(b) shows the distribution of decay times.

In conclusion, we have demonstrated high resolution spectroscopy of the $^1S_0 \rightarrow ^3P_0$ clock transition in $^{27}\text{Al}^+$ using quantum logic. This technique was used to measure the clock transition frequency with a fractional uncertainty of 5×10^{-15} . We have also calibrated the g factors of the 1S_0 and 3P_0 states and measured the 3P_0 state lifetime. These are the basic steps necessary to implement an accurate frequency standard based on $^{27}\text{Al}^+$.

P.O.S.'s work was supported by the Alexander von Humboldt Foundation. J.C.J.K.'s work was supported by the Netherlands Organisation for Scientific Research. We acknowledge support from ONR and DTO. We thank V. Meyer for constructing the ion trap used for these experiments and E.A. Donley, J. Ye, M.A. Lombardi, and D.R. Smith for their careful reading of this manuscript. The authors are grateful to T.E. Parker, S.R. Jefferts, and T.P. Heavner for providing the absolute frequency calibration. This work is a contribution of NIST and is not subject to U.S. copyright.

[†]Present address: Institut für Experimentalphysik, Universität Innsbruck, Austria.

[‡]Present address: School of Mechanical Engineering, Yonsei University, Seoul, Korea.

[§]Present address: Institut für Experimentalphysik, Heinrich-Heine-Universität Düsseldorf, Germany.

- [1] H.G. Dehmelt, IEEE Trans. Instrum. Meas. **31**, 83 (1982).
- [2] N. Yu, H. Dehmelt, and W. Nagourney, Proc. Natl. Acad. Sci. U.S.A. **89**, 7289 (1992).
- [3] T. Rosenband *et al.*, arXiv:physics/0611125.
- [4] J.I. Cirac and P. Zoller, Phys. Rev. Lett. **74**, 4091 (1995).
- [5] D.J. Wineland *et al.*, in *Proceedings of the 6th Symposium on Frequency Standards and Metrology*, edited by P. Gill (World Scientific, Singapore, 2002), pp. 361–368.
- [6] P.O. Schmidt *et al.*, Science **309**, 749 (2005).
- [7] S.A. Diddams *et al.*, Phys. Rev. Lett. **84**, 5102 (2000).
- [8] T. Udem, R. Holzwarth, and T.W. Hänsch, Nature (London) **416**, 233 (2002).
- [9] W.M. Itano *et al.*, Phys. Rev. A **47**, 3554 (1993).
- [10] J.E. Bernard, L. Marmet, and A.A. Madej, Opt. Commun. **150**, 170 (1998).
- [11] M.A. Rowe *et al.*, Quantum Inf. Comput. **2**, 257 (2002).
- [12] C. Monroe *et al.*, Phys. Rev. Lett. **75**, 4011 (1995).
- [13] D.B. Hume *et al.* (to be published).
- [14] Q.A. Turchette *et al.*, Phys. Rev. A **61**, 063418 (2000).
- [15] L. Deslauriers *et al.*, Phys. Rev. Lett. **97**, 103007 (2006).
- [16] M.D. Barrett *et al.*, Phys. Rev. A **68**, 042302 (2003).
- [17] W. Nagourney, N. Yu, and H. Dehmelt, Opt. Commun. **79**, 176 (1990).
- [18] W.M. Itano (to be published).
- [19] T.M. Fortier, A. Bartels, and S.A. Diddams, Opt. Lett. **31**, 1011 (2006).
- [20] T.E. Parker, S.R. Jefferts, T.P. Heavner, and E.A. Donley, Metrologia **42**, 423 (2005).
- [21] T.E. Parker (private communication).
- [22] M.M. Boyd *et al.*, Science **314**, 1430 (2006).
- [23] M.G.H. Gustavsson and A.-M. Mårtensson-Pendrill, Phys. Rev. A **58**, 3611 (1998).
- [24] D.J. Wineland, J.J. Bollinger, and W.M. Itano, Phys. Rev. Lett. **50**, 628 (1983).
- [25] P. Raghavan, At. Data Nucl. Data Tables **42**, 189 (1989).
- [26] T. Brage, P.G. Judge, A. Aboussaid, M.R. Godefroid, P. Jönsson, A. Ynnerman, C.F. Fischer, and D.S. Leckrone, Astrophys. J. **500**, 507 (1998). These results contain a typographical error. The $\text{Al}^+ ^3P_0$ lifetime listed in Table 6 is 377 s, but the result obtained from the formula in the inset in Fig. 3 is 19.5 s, which is close to the observed value.
- [27] E. Peik, G. Hollemann, and H. Walther, Phys. Rev. A **49**, 402 (1994).
- [28] D.J. Wineland *et al.*, J. Res. Natl. Inst. Stand. Technol. **103**, 259 (1998). These fluctuations stem from the statistical distribution of motional states during Doppler cooling. The calculated damping rate is slightly larger than the observed rate, because some fluctuations average away when the $^{27}\text{Al}^+$ ion is continuously cooled during interrogation.

*Electronic address: trosen@boulder.nist.gov